

Geomechanical Evaluation of an onshore oil field in the Niger Delta, Nigeria

Fidelis Ankwo Abijah¹, Akaha Celestine Tse²
^{1,2}Department of Geology, University of Port Harcourt, Nigeria

Abstract: Wellbore failure reportedly accounts for more than 10% of drilling non productive time in the Niger Delta. Rock mechanical properties critical to wellbore stability, well design, fracking, sanding prediction and production planning were evaluated in 3 wells in an onshore field, western Niger Delta using 4-arm caliper, gamma ray, density and sonic logs, leak off tests and seismic data in an onshore field, Eastern Niger Delta. The stratigraphic units between 2000 and 3000 m depth investigated are the typical interlayered, normal to abnormal pressured shales and sandstones of the Agbada Formation. Wellbore breakouts were predominant in shales and weak shaly sandstones across the lithologic units. The vertical stress magnitude ranges from 23.08 - 25.57 MPa/km, minimum effective horizontal stress from 13.80 - 14.03 MPa/km, and maximum effective horizontal stress from 16.06 - 17.65 MPa/km inferring a normal fault stress regime. The minimum horizontal stress orientation varies from 015° - 033° forming the most stable azimuth for geosteering a directional well while the maximum horizontal stress orientation is N60°E - N123°E which is in agreement with the regional fault orientations in the Niger Delta. ENE – WSW, WNW – ESE and other maximum horizontal stress orientations suggest multiple sources of stress and in situ stress rotation across faults suggests wellbore instability. Structural evolution depicts NE – SW and NW-SE trending faults in the direction of the maximum horizontal stress. These data will be useful in the planning of well drilling in the field.

Keywords: azimuth, breakout, geomechanical, stresses, wireline logs, Niger Delta.

I. Introduction

Oil and gas field development planning requires placing wells correctly, whether vertical, deviated or horizontal in order to maintain a safe and stable wellbore and achieve optimum production. [1] reported that common oil production problems in the Niger Delta includes water coning, wellbore instability, sand production, wax deposition and high gas/oil ratios. Geomechanical analysis and modeling are tools employed to generate data for the design of a stable wellbore. Drilling a borehole in the earth introduces fluids into a stable formation causing formation pressure changes, re-orientation of in situ stresses and concentration of stresses on the wellbore wall creating a differential between the wellbore and far field stresses that could exceed rock strength and causing failure. This phenomenon is responsible for several changes that can result in wellbore instability, poor hydraulic fracture initiation and propagation, casing collapse, perforation failure, sanding, sub-optimal production, fault reactivation amongst others [2, 3, 4]. Geomechanical properties of reservoir rock include Poisson's ratio, total minimum horizontal stress, and bulk, Young, and shear modulus. Principal stress profile of an oil and gas reservoir depends highly on the rock geomechanical properties. Geomechanical evaluation, modeling and monitoring enables predicting and mitigating the effects of stress and pressure changes and the resultant strains on the reservoir, wellbore and completion in the formation. Having access to geomechanical data can assist engineers and geoscientists during geomechanical modeling, hydraulic fracture treatment design, and reservoir simulation in hydrocarbon fields [5,6]. The magnitude and orientation of the stresses, their effect on the rock properties and wellbore and their impacts on the field under the in situ stress regime are fundamental in predicting and managing rock deformation through design, drilling and production to prevent drilling problems.

Wellbore instability indicators includes breakout, collapse, undergaged hole, cavings at surface, excessive volume of cuttings and cavings, increased circulating pressures, unscheduled sidetracks, or even abandonment etc [7, 8, 9, 10, 11]. Designing and maintaining a stable wellbore requires acquisition of geomechanical properties data from drilling cores or from wireline logs [12, 13]. Using wireline logs for estimating geomechanical properties of rocks achieves satisfactory results because the logs are always run in the entire section of reservoir rocks. They give direct measurements of the petrophysical properties, and hence have become an ideal medium for obtaining geomechanical data [14]. Core samples of overburden formations where compressive shear failures occur, give better results but are never available for testing prior to commencement of drilling. In order to predict and design a solution to these problems, geomechanical evaluation and modeling are performed based on empirical correlations from measurable physical properties obtainable from wireline logs normally available for all offset wells within the field for pre-drilling analysis, modeling and design [3, 15].

These empirical relations are derived based on the fact that the factors that affect the formation parameters such as velocity, porosity and elastic moduli equally affect rock strength and other geomechanical properties.

The high costs and complexity of wells both in terms of geometry, high-pore-pressure, low permeability, anisotropic and high stress regimes demand proactive pre-design geomechanical modeling of rock strength, deformation and stress for economic success of field developments. It is estimated that the minimum cost of instability of wells in the Niger Delta is 10% of the total cost per year, also the cost of non-productive time during drilling varies from a minimum of 60 days and sometimes up to 140 days with shales accounting for 90% of instability [16]. Poor understanding of a field's geomechanics including the rock elastic properties, rock strength, in situ stress and wellbore stresses around the wellbore wall is a major contributory factor to poor well design and suboptimal production leading to collateral problems including severe wellbore collapse, lost circulation, blow outs, sidetracking and even well abandonment especially in directional and extended reach wells. This demands wellbore stability analysis during the planning phase of a field. This study is aimed at carrying out geomechanical and wellbore stability analysis of wells in a field in the Niger Delta to determine rock mechanical properties for geosteering a stable wellbore, hydraulic fracture orientation in directional wells and general pre-drilling planning.

II. Geologic Setting

The study field is located in the onshore coastal swamp of the Niger Delta basin (Fig. 1). The tectonic evolution of the Niger Delta was controlled by Cretaceous fracture zones formed during the triple junction rifting and opening of the south Atlantic. The stratigraphic succession in the basin consists of three lithostratigraphic units. The oldest unit is the basal Akata Formation, Paleocene to Holocene in age and comprising shales thought to be the source rock, was deposited under marine conditions. The Akata is overlain by the paralic sandstone/shale layers of the Agbada Formation which is the reservoir rock. Capping the sequence is the continental sand and sandstones of the Benin Formation which is the regional aquifer. These rock units are time transgressive, and they range in age from Tertiary to Recent [17]. Petroleum reservoirs in the Niger Delta are basically sandstone and unconsolidated sands in the Agbada Formation. The primary seal rocks are the interbedded shales within the Agbada Formation. Both structural and stratigraphic traps are common. The structural traps consist of growth faults and roll over anticlines which developed during syndimentary deformation of the Agbada paralic sequence due to the instability of the under-compacted, over-pressured Akata shale [18, 19]. The interbedded shale within the Agbada Formation provides sealing units.

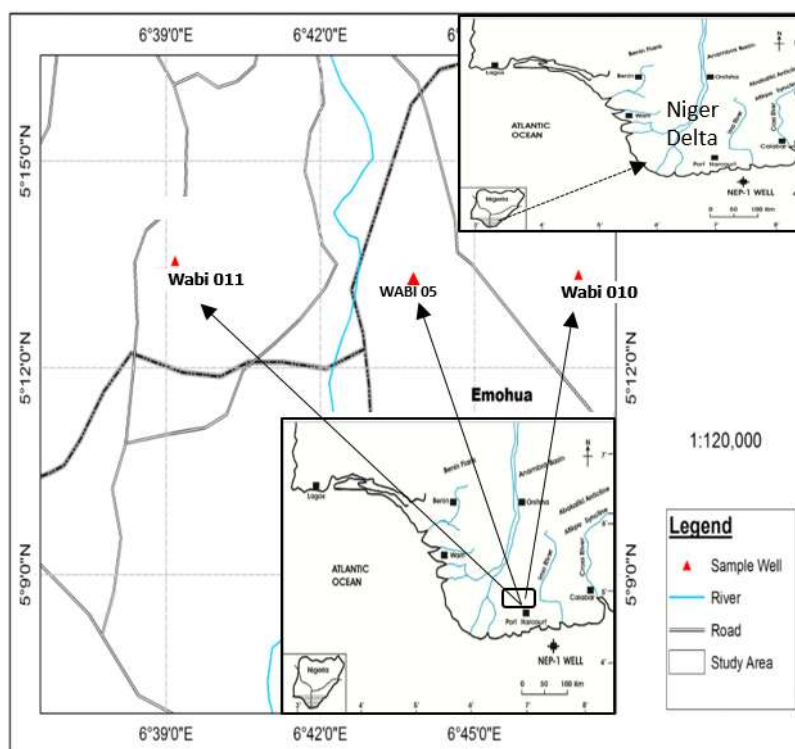


Figure 1: Map of the study area.

III. Methods Of Study

Data for this study included wireline logs (sonic, density, gamma ray, resistivity, and neutron porosity logs), 3D seismic data and Leak off tests (LOT) for 3 wells codenamed WABI 05, 010 and 011 for proprietary reasons. The wells lie in an east-west direction. These were available in well log American Standard Code for Information Interchange (ASCII) standard files formats. They were subjected to quality checks and converted to true vertical depth and thereafter loaded into the Schlumberger Petrel 2011 software to analyse and isolate the breakout zones. Stress induced wellbore failure zones known as breakouts were isolated from non-stress induced wellbore enlargements such as keyseats and washouts using 4-arm caliper and gamma ray log using the criteria for their identification in a well as outlined by [20, 21, 22]. Determination of rock mechanical properties including elastic and inelastic properties was carried out using density and sonic compressional (ΔT_c) and shear (ΔT_s) transit times as described in detail by [23, 6, 14]. The elastic properties included Poisson ratio (ν), elastic modulus (E) shear/rigidity modulus (G), bulk and matrix/grain moduli (K_b and K_m), bulk and grain compressibility (C_b and C_r), and Biot's coefficient. The inelastic properties determined were fracture gradient and rock strength which include Uniaxial compressive strength, tensile and cohesive strengths, and frictional angle. Poisson's ratio and Young's Modulus (E), Shear Modulus (G), Bulk Modulus (K_b) and Matrix/Grain Bulk Modulus (K_m) were obtained from the wireline logs using empirical relationships as described by [24, 25, 26]. Poisson's ratio and Young's modulus were determined from P- and S- wave velocity.

Where shear transit times data were not available like in well Wabi 05, interval transit time of the shear wave (ΔT_s) was estimated and used to derive the shear wave velocity (V_s). This was achieved using the [27] relationships in equations (1), (2), and (3).

$$V_p = \frac{304878}{\Delta T_c} \quad (1)$$

$$V_s = \frac{304878}{\Delta T_s} \quad (2)$$

$$V_s = (0.804 \times V_p) - 0.856 \quad (3)$$

Poisson Ratio (ν)

Poisson ratio (ν) was computed from acoustic measurements including the slowness of the compressional wave (ΔT_c) and shear wave (ΔT_s) ratio using the [28] and [2] methods (equation 4) expressed as

$$\nu = 0.5 \left(\frac{V_p}{V_s} \right)^2 - \frac{1}{\left(\frac{V_p}{V_s} \right)^2} - 1 \quad (4)$$

Shear Modulus (G)

The shear modulus (G) which is the ratio of the shear stress to the shear strain was estimated from the [29] formula (equation 5)

$$G = \frac{a \rho_b}{\Delta T_{sv}} \quad (5)$$

where coefficient $a = 13464$, ρ_b = bulk density, ΔT_s = shear sonic transit time.

Bulk Modulus (K_b)

The bulk modulus (K_b) was computed from the sonic and density logs using equation 6

$$K_b = a \rho_b \left(\frac{1}{\Delta T_{c2}} - \frac{4}{3 \Delta T_{s2}^2} \right) \quad (6)$$

where ΔT denotes sonic transit times for compressional and shear waves.

Matrix/Grain Bulk Modulus (K_m)

This was determined from the empirical relationship in equation 7

$$K_m = KS \rho_{ma} / (1/\Delta T_{Cma}^2 - 4/3 \Delta T_{Sma}^2) \quad (7)$$

Young's Modulus (E)

Young's modulus or modulus of elasticity was determined from shear modulus and Poisson's ratio as in equation (8).

$$E = 2G (1 + \nu) \quad (8)$$

Bulk Compressibility (C_b) with porosity was determined by the relationship in equation 9

$$C_b = 1/K_b \quad (9)$$

Rock Compressibility (C_r) zero porosity was obtained from equation 10 as

$$C_r = 1/(a \rho_{log} (1/\Delta T_{Cma}^2 - 4/3 \Delta T_{Sma}^2)) \quad (10)$$

Biot Constants

Biot's poroelasticity describes the coupling between pore pressure and stress in rocks. When pore pressure changes and stresses are coupled, fluid diffusion plays an important role making stability time-dependent [30] Biot constant (α) was determined from the [31] method in terms of bulk and grain modulus using the expressions in equations 11 and in terms of compressibility (equation 12) as

$$\alpha = 1 - K_b/K_m \quad (11) \quad \text{where}$$

K_b and k_m are skeleton bulk and solid grain moduli respectively

$$\alpha = 1 - C_r/C_b \quad (12)$$

where C_r and C_b are grain and bulk compressibility respectively.

Unconfined Compressive Strength (UCS)

Among the several empirical relationships proposed for application in sandstones, shales and carbonate rocks, the [32]relationship (equation 13) for fine grained, consolidated and unconsolidated sandstones with all porosity ranges suitable for the Niger Delta was adopted while [33] equation for shales was used for comparison of results as in equation 14.

$$UCS = 1200 \exp^{(-0.036\Delta Tc)} \tag{13}$$

$$UCS = 10(304.8/\Delta Tc - 1) \tag{14}$$

where UCS = unconfined compressive strength, ΔTc = compressional wave transit time.

Shear Strength

The initial shear strength (τ_i) and in situ rock's tensile strength (T_o) were determined using the empirical relationships by [34] in equation 15

$$\tau_i = 0.026E/C_b \times 10^6 \{0.008V_{sh} + 0.0045(1-V_{sh})\} \tag{15}$$

where E = Elastic modulus, C_b = bulk compressibility and V_{sh} = volume of shale and

$$\text{Insitu rock Tensile strength, } T_o = C_o/12 \tag{16}$$

where C_o = cohesive strength = $5(V_p - 1)/0.5(V_p)$

Determination of in situ stresses magnitudes and orientation

Vertical stress (σ_v) was determined by integrating the density (ρ_b) of the materials from surface to the depth of interest as in equation 17 where

$$\sigma_v = \int^z \rho_b(z) g dz \tag{17}$$

The poroelastic equation which shows the relationship between vertical stress and minimum horizontal stress, Poisson's ratio and pore pressure (p_w) was used together with leak off test to calculate the minimum horizontal stress (σ_H) according to equation 18

$$\sigma_H = K (\sigma_v - \alpha p_w) + \alpha p_w \tag{18}$$

Where α is Biot's coefficient and p_w is mud pressure.

Maximum horizontal stress (S_{Hmax}) was calculated using the [11]relationship in equation 19

$$S_{Hmax} = S_{hmin} + t_f(SV - S_{hmin}) \tag{19}$$

Where t_f is tectonic factor. The direction of S_{Hmax} was measured from the existing borehole breakout data.

The orientation of maximum and minimum horizontal stresses was interpreted from wellbore breakouts and drilling induced tensile fractures using formation image logs and from breakout analysis using multi arm caliper logs as described by [35 and 22] Using the criteria proposed by [20] and [36]. Breakout data were ranked in accordance with the World Stress Map quality ranking system [22]. Breakout orientation data were analyzed statistically using equations by [37] and data ranked after the World Stress Map breakout quality ranking system described by [38].

Fracture gradient

[39] distinguished between fracture gradient which is practically the minimum horizontal stress and the most likely fracture gradient during drilling as presented (equation 20)

$$P_{FP} = \frac{3v}{2(1-v)(\sigma_v - \alpha P_p)} + \alpha P_p \tag{20}$$

where P_{FP} = most likely fracture pressure gradient, σ_v = vertical stress, α = Biot's constant, P_p = pore pressure gradient.

Minimum mud weight

Wellbore stability analysis was carried out by determining the minimum and maximum mud weights required to prevent compressive shear failure and unwanted tensile fracturing. The minimum mud weight, the collapse pressure or shear failure gradient is the pressure required to drill safely below which shear failure will occur causing breakout and instability. It is derived from the [29] formula in equation 7 based on Mohr-Coulomb criterion for critical wellbore pressure which is

$$P_c = \{1.5 \sigma_{Hmax} - 0.5 \sigma_{hmin} \alpha p_p (1-2\nu/1-\nu) - 1.732\tau_i\} / 1 - 0.5\alpha(1-2\nu/1-\nu) \tag{21}$$

where τ_i the initial shear strength

$$\tau_i = \frac{0.026E}{C_b} \times 10^6 \{0.008V_{sh} + 0.0045(1-V_{sh})\} \tag{22}$$

where E = Elastic modulus C_b = bulk compressibility, V_{sh} = volume of shale, ν = Poisson ratio, α = Biot's coefficient, σ_{Hmax} = maximum horizontal stress, σ_{hmin} = minimum horizontal stress and p_p = Pore pressure

IV. Results And Discussion

The studied rocks interval range in depth from 2 to 4km in the subsurface. It falls within the Agbada Formation whose stratigraphic succession consists of interbedded sandstones and shales. A correlation of the lithologic logs of the 3 wells delineated eight reservoir sand units labelled A to Has shown in Fig. 2. Typical

elastic and rock strength properties derived from empirical relations are summarized in Tables 1 and 2. The mechanical properties of the rocks are displayed on the well logs in Fig. 3 showing variation of the elastic properties, the rock strength and volume of shale. There are significant variations in properties between the cap rocks and the reservoir sand units across the field (Table 3). The cap rock which is shale, has high average Poisson ratio, elastic, bulk and rigidity moduli of 0.40, 23,466.1 MPa, 253,312.8 MPa, and 8,717 MPa, respectively. However, lower bulk compressibility and rock strength make the shale more ductile, stiffer, less compressible and more prone to compressive shear failure (Fig. 4), but better fracture stimulation barriers. Conversely, sandstones, the main reservoir rocks, have relatively lower Poisson ratio, elastic, bulk and rigidity moduli but higher compressibility and rock strength making them more brittle (Fig. 5) with higher potential for tensile failure. Thus, sandstone will fracture before shales in a hydraulic fracture stimulation process under the same fracture gradient while shales will form the barrier to fracture growth. Low rock strength accounts for the occurrence of wellbore failures in shales and weak shaly sandstones. Correlation of the properties across the field shows higher values of elastic, bulk and rigidity moduli in the east. Lateral decrease in the magnitude of the rigidity modulus from WABI 10 well on the eastern flank to WABI 11 well on the west implies a decrease in present day deformation eastward. There is a general decreasing trend in the modulus of rigidity, bulk and matrix moduli and an increase in elastic modulus of the rocks with depth.

Compaction equilibrium during diagenesis under anoxic conditions depicted by normally pressured shale source beds favoured hydrocarbon accumulation with the shale smears on the faults and caps on the sand tops providing the traps. The increase in rock compressibility with effective vertical stress and effective porosity and decrease in compressibility with depth and decrease in effective porosity with bulk compressibility further support equilibrium compaction. Increase in effective overburden stress due to sediment loading and fluids expulsion causes grain sliding in shear and compactional deformation with reduction in the bulk and grain compressibility and pore volume of the sediment with increasing depth. Grain to grain contact destroys the cement bonds and closes packing of individual grains by elastic distortions and strains. This mechanism is responsible for generation of over pressures since impermeable sediments such as shales saturated with an incompressible fluid will not deform elastically and when there is disequilibrium compaction, abnormal pore pressures will form as reported in most fields in the Niger Delta [40, 41]. Young tertiary sedimentary rocks deform primarily by compaction resulting in progressive loss of porosity with increasing depth of burial [42].

In Situ And Wellbore Stress Magnitude

The in situ and wellbore stress magnitudes (Table 4) are displayed on the logs in Fig. 6. These vertical stress gradients indicate a variation across the field with magnitudes ranging from 23.08 MPa/km at 2km to 25.57 MPa/km at 4km in WABI 10, to 21.50 MPa/km at 2km to 22.63 MPa/km in WABI 11. There is a general increase in vertical stress with depth of burial due to increase in overburden loading. The magnitudes of the maximum and minimum horizontal stresses follow the trend of the vertical stress. Estimating the minimum horizontal stress in a well provides the lower limit of the fracturing pressure and puts a limit on the allowable injection pressure in a well. While the minimum horizontal stress varies from 14.03 MPa/km at 2km to 14.48 MPa/km at 4km true vertical depth s, the maximum horizontal stress ranges from 17.65 MPa/km at 2km to 16.06 MPa/km at 4km. The decrease in maximum horizontal stress magnitudes with depth of burial is due to variations in the bulk densities of the subcrustal rocks across the delta with a gradual increasing trend in easterly direction. Variations in crustal rock bulk density across the field could be caused by the deposition of siliciclastic materials derived from weathering of rocks in the hinterland during the rifting and uplift of the adjoining lower Benue Trough in the Late Jurassic to the Middle Cretaceous [43]. This was accompanied by post rifting gravity tectonic deformation and induced deformation due to shale mobility during depositional episodes [1]. Variation in vertical stress magnitude, pore pressure and the tectonic stress factor also accounts for the differences in the magnitudes of the horizontal stresses [44].

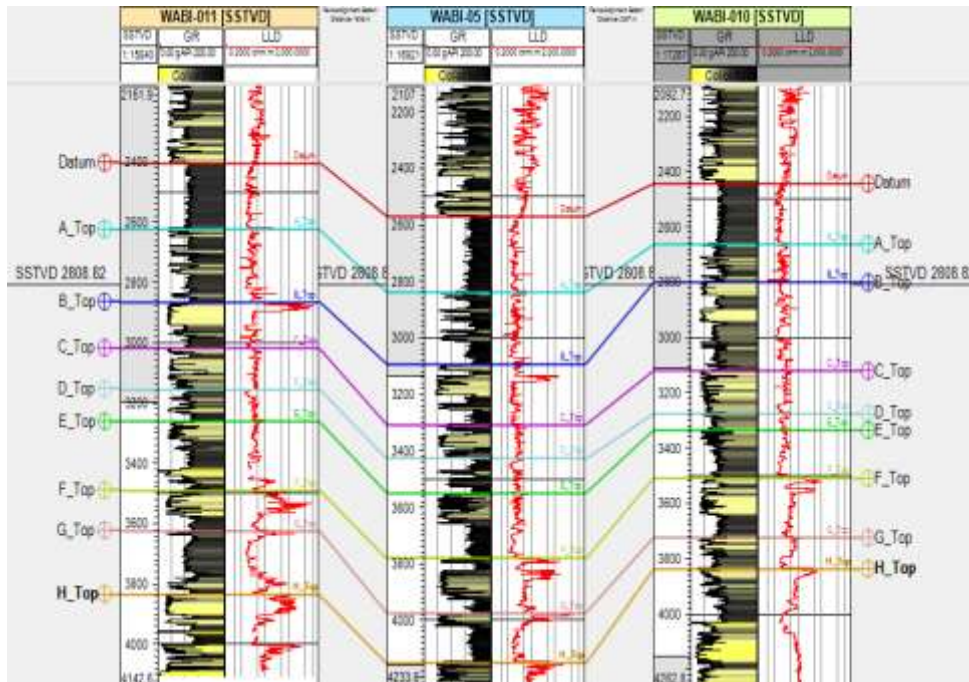


Figure 2 Litho-correlation of the wells showing the reservoirs

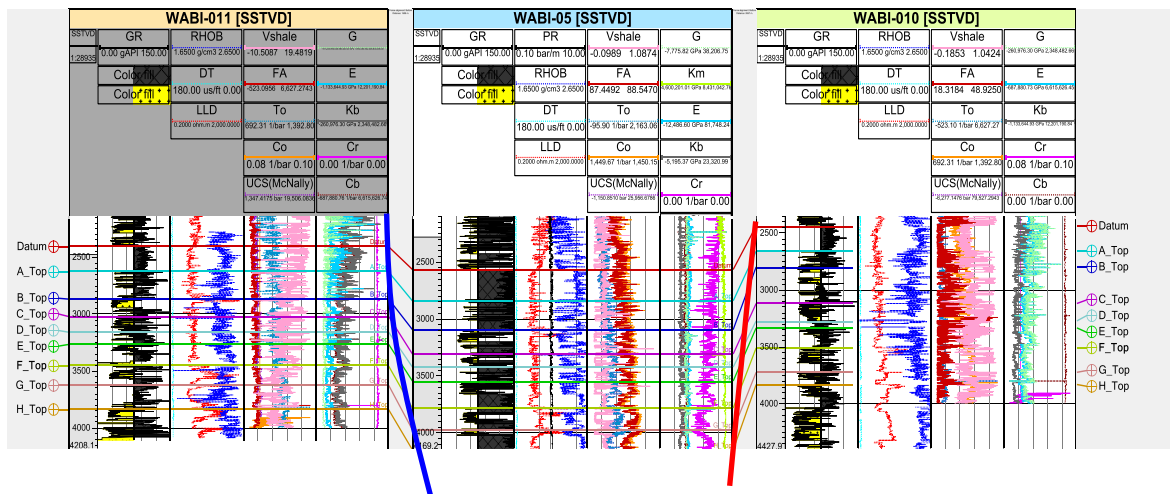


Fig. 3 Mechanical properties of the rocks shown on the logs..

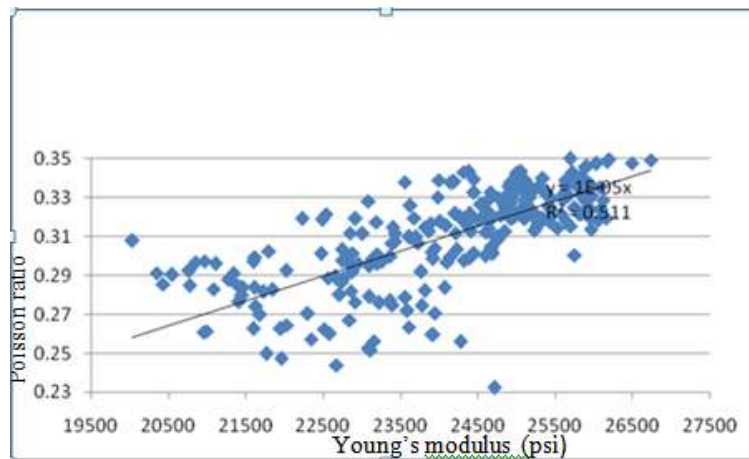


Figure 4 Young's modulus vs Poisson ratio plot for WABI 05 well showing sandstone brittleness and shale ductility

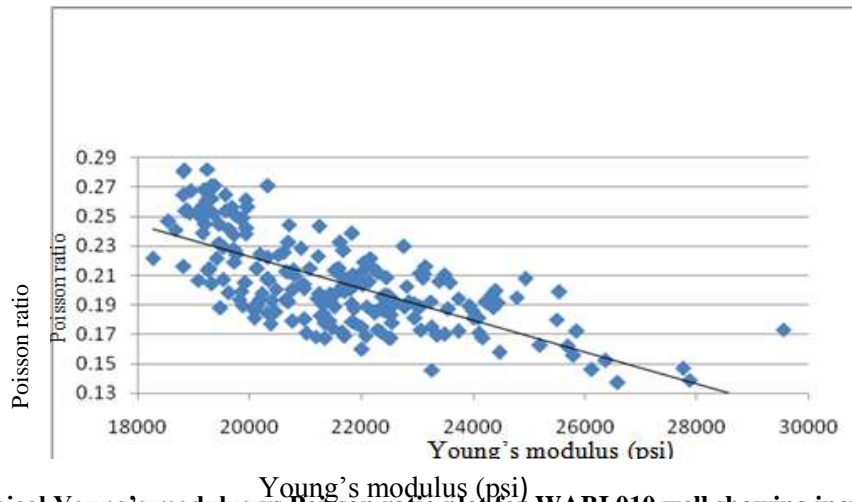


Figure 5 Typical Young's modulus vs Poisson ratio plot for WABI 010 well showing increasing sandstone brittleness with decreasing clay content

Table 1. Rock elastic properties

Well	Depth (m)	Rock type	v	K _o	G (Mpa)	K _b (Mpa)	K _m (Mpa)	E (Mpa)	C _b (Mpa)	C _r (Mpa)	α
WABI 10	2000	Sh	0.33	0.49	7000.77	18,455.3		18,644.8	2.58 x 10 ⁻⁹	5.96 x 10 ⁻⁴	1
	2500	Sh	0.34	0.52	8,717.91	253,312.8		23,466.1	1.87 x 10 ⁻⁹	5.96 x 10 ⁻⁴	1
	3000	Sh	0.33	0.50	7,262.97	19,500		19,382.5	2.44 x 10 ⁻⁹	5.96 x 10 ⁻⁴	1
	3500	Sst.	0.21	0.27	2,877.3	4,112.19		7,003.8	1.15 x 10 ⁻⁹	5.96 x 10 ⁻⁴	1
	4000	Sst.	0.27	0.37	4,845.13	8,947.59		12,312.9	5.31 x 10 ⁻⁹	6.0 x 10 ⁻⁴	1
WABI 05	1500	Sh	0.35	0.52	69.8	188.4	18.86	53,037.6	2.52 x 10 ⁻⁶	2.45 x 10 ⁻⁴	0.9
	2000	Sh	0.34	0.52	69.38	186.4	19.43	51,412.95	3.54 x 10 ⁻⁴	-3.1 x 10 ⁻³	0.9
	2500	Sh/Sst	0.33	0.48	68.13	180.99	20.72	54,769.9	3.33 x 10 ⁻³	-9.65 x 10 ⁻²	0.9
	3000	Sst.	0.26	0.35	58.86	148.42	23.68	55,167.5	2.91 x 10 ⁻³	-1.31 x 10 ⁻⁷	0.9
	3500	Sst.	0.22	0.29	58.99	145.1	26.13	55,413.4	2.64 x 10 ⁻³	-1.72 x 10 ⁻⁷	0.9
	4000	Sst.	0.27	0.37	59.96	152.49	23.22	55,390.5	2.97 x 10 ⁻³	-0.0344	0.9
WABI 11	1500	Sh	0.37	0.60	2.43 x 10 ⁻⁶	5.5 x 10 ⁻¹⁰	51,169.5	6.69 x 10 ⁻⁹	86,773.1	5.95 x 10 ⁻⁴	1
	2000	Sh	0.35	0.55	3.3 x 10 ⁻⁹	8.8 x 10 ⁻⁹	51,745.4	9.03 x 10 ⁻⁹	545,787.1	5.95 x 10 ⁻⁴	1
	2500	Sh/Sst	0.32	0.47	5.6 x 10 ⁻⁹	1.7 x 10 ⁻⁹	54,790.7	1.47 x 10 ⁻⁸	27,320.3	5.95 x 10 ⁻⁴	1
	3000	Sst.	0.27	0.37	9.2 x 10 ⁻⁹	4.7 x 10 ⁻⁹	55,206.9	2.34 x 10 ⁻⁸	13,380.6	5.95 x 10 ⁻⁴	1
	3500	Sst.	0.25	0.33	1.1 x 10 ⁻⁹	6.2 x 10 ⁻⁹	55,143.1	2.89 x 10 ⁻⁸	9,992.7	5.96 x 10 ⁻⁴	1
	4000	Sst.	0.18	0.23	1.2E-8	6.2 x 10 ⁻⁹	48,914.4	2.96 x 10 ⁻⁸	7,749.2	5.96 x 10 ⁻⁴	1

Sh = shale Sst = sandstone v = Poisson's ratio, G = Modulus of rigidity, E = Young's modulus, k_b = Bulk modulus, K_m = Bulk modulus C_b = Bulk compressibility, C_r = Volume compressibility, α = Biot coefficient

Table 2: Rock strength profile across the wells

Well	Depth(m)	Rock strength parameters							Petrophysical parameters	
		Rock type	UCS MPa	C _o MPa	T _o MPa	τ _i MPa	F _A (NPHI) (deg)	F _A (V _p) (deg)	V _{sh} (frac)	Φ _{eff} (frac)
WABI 10	2000		24.95	6.45	2.08	8.60	28.0	14.5	0.60	0.22
	2500		20.68	6.51	1.72	1.99 x 10 ¹⁵	20.87	15.5	0.27	0.10
	3000		23.99	6.78	1.99	1.43 x 10 ¹⁵	27.11	14.8	0.54	0.20
	3500		89.03	6.89	7.42	1.05 x 10 ¹⁵	22.02	0	0.43	0.07
	4000		53.06	7.52	4.42	3.99 x 10 ¹⁴	20.8	7.4	0.42	0.0008
WABI 11	1500		20.21	5.8	1.68	7.17 x 10 ⁻¹⁴	22	16	0.19	0.26
	2000		24.78	6.14	2.06	1.95 x 10 ⁻¹³	22	17	0.59	0.23
	2500		32.11	6.59	2.69	4.51 x 10 ⁻¹³	33	13	0.05	0.10
	3000		38.79	7.14	2.89	1.78 x 10 ⁻¹³	22	7	0.33	0.12
	3500		78.44	7.35	6.64	3.4 x 10 ⁻¹³	28	4	0.64	0.09
	4000		57.33	7.45	4.78	5.19 x 10 ⁻¹³	22	2	0.59	0.17
WABI 10	2000		15.39	9.99	1.28	5.52 x 10 ⁻⁵	ND	87	0.02	0.25
	2500		28.84	10.34	2.40	5.0 x 10 ⁻⁷	ND	87	0.11	0.33
	3000		52.32	10.34	4.36	4.27 x 10 ⁻⁷	ND	88	0.17	0.09
	3500		67.22	9.99	5.60	4.5 x 10 ⁻⁷	ND	88	0.05	0.21
	4000		57.13	9.99	4.76	4.93 x 10 ⁻⁷	ND	88	0.24	0.11

UCS = Unconfined compressive strength, C_o = Cohesion, T_o = Tensile strength, τ = Shear stress, F_A = Angle of friction, V_{sh} = Volume of shale Φ_{eff} = Effective porosity ND = not determined

Orientation Of The Horizontal Stresses.

The wellbore breakout orientation data in Fig. 7 indicating the breakout zones and relative bearing data Table 5) imply that compressive shear failure was dominant in shales and weak shaly sandstones. This shows that failure is lithology independent, rather, it depends on the rock strength, degree of compaction and in situ stress concentration. Therefore, low rock strength accounts for the occurrence of wellbore failures in shales and weak shaly sandstones evident on the breakout logs. Breakout azimuths plotted on Rose diagram shown in Fig. 8 consists of breakout zones with more than 4 orientations. These fall in the World Stress map breakout quality classes A and C [22, 38] are ranked as breakouts of acceptable quality. The minimum horizontal stress azimuth ranges from $015^\circ - 033^\circ$ while the maximum horizontal stress orientation is $N60^\circ E - N123^\circ E$. Breakouts in the wells show orientation of the maximum horizontal stress in the ENE – WSW, NNW – SSW, NW – SE directions which suggest multiple sources of stress. The ENE – WSW orientation is parallel to the Romanche fracture zone and the NE – SW orientations of the regional fault in the Niger Delta have been suggested as the major lines of weaknesses separating the North and South Atlantic [45]. The structural style of the field infers a NW-SE and NE-SW trending fault (Fig.3) consistent with the direction of the maximum horizontal stress. This indicates that WABI 05 well was the infilling depocenter and WABI 11 and 10 wells are upthrown blocks. [46] have suggested that repeated earth tremors are the effects of continental crust reactivation linking the onshore faults along major lineaments.

Table 3 Comparison of rock mechanical properties of wellbore breakout zones and in-gauge sections.

Parameter	Breakout zone		In gauge section
Rock type	Shale	Sandstone	Shale /sandstone
Poisson ratio	0.34 – 0.40	0.220 - 31	0.12 – 0.35
Elastic modulus (MPa)	12,990.1 – 78,508.4	16,131.51 – 22,351.44	8,639.74 – 40,915.03
Rigidity modulus (MPa)	5,068 – 27,158.9	6,150.71 – 8509.57	-4.69E-5 – 27,158.2
Bulk modulus (MPa)	$8.8 \times 10^{10} - 37,308.7$	14,251.89 – 25,351.44	3374.6 – 14,537.9
Grain modulus (MPa)	18.86 – 55,206.9	-	4394.0 – 76,221.6
Bulk compressibility (MPa)	$2.58 \times 10^{-9} - 545,787.1$	$1.88 \times 10^{-9} - 3.34 \times 10^{-9}$	$2.62 \times 10^{-9} - 3.63 \times 10^{-8}$
Grain compressibility (MPa)	$-9.65 \times 10^{-8} - 6.0 \times 10^{-4}$	$5.95883 - 5.95884 \times 10^4$	$-46.75 - 5.96 \times 10^4$
Unconfined Compressive strength (Mpa)	2.23 – 44.0	19.21 – 32.86	45.0 – 1200.3
Cohesive strength (Mpa)	7.0 – 7.4	6.4229 – 6.67442	7.2 – 42.8
Shear strength(initial) (Mpa)	$4.74 \times 10^{-8} - 7.07 \times 10^{15}$	$9.51 \times 10^{14} - 2.41 \times 10^{15}$	$2.0 \times 10^{15} - 7.1 \times 10^{16}$
Tensile strength (Mpa)	0.19 – 3.92	1.60144 – 2.7387	3.0 – 41.0
Friction angle (deg.)	2.90 – 15.83	12.65 – 15.82	7.4 - 88
Fracture gradient (Mpa/km)	11.53 – 16.4	13.07 – 14.65	9.0 – 18.4

Table 4 Typical in situ and wellbore stress profile

Well No	Depth (m)	Far field stress			Wellbore stresses			
		Vertical stress (σ_v) (MPa/km)	Maximum horizontal stress (σ_{Hmax}) (MPa/km)	Minimum horizontal stress (σ_{Hmin}) (MPa/km)	Maximum Hoop stress ($\sigma_{\theta\theta}^{max}$) (MPa/km)	Minimum hoop stress ($\sigma_{\theta\theta}^{min}$) (MPa/km)	Maximum axial stress (σ_{zz}^{max}) (MPa/km)	Minimum axial stress (σ_{zzmin}) (MPa/km)
Wabi 10	2000	23.08	17.65	14.03	15.84	11.99	25.57	20.59
	2500	23.53	15.61	14.03	16.97	21.95	26.48	22.18
	3000	22.86	16.52	14.96	19.24	20.82	23.31	20.82
	3500	23.54	16.29	14.48	22.40	1.36	24.21	22.86
	4000	25.57	16.07	14.48	20.59	-0.68	29.42	21.72
Wabi 11	1500	21.05	17.65	15.38	24.44	4.53	22.85	19.46
	2000	21.50	18.10	14.93	24.89	4.07	19.91	19.91
	2500	23.54	14.93	12.67	24.44	3.17	22.18	21.95
	3000	23.54	14.93	12.67	24.44	3.17	22.18	21.95
	3500	23.99	15.39	11.99	25.57	2.72	22.40	22.18
4000	22.63	12.45	12.22	19.46	2.94	21.95	21.95	
Wabi 05	2000	21.90	19.24	14.94	37.33	13.57	22.63	18.56
	2500	20.14	19.46	15.39	38.01	12.89	22.85	15.84
	3000	23.30	16.75	13.58	29.87	14.03	26.25	22.17
	4000	23.76	14.94	11.32	33.03	7.46	22.63	21.72

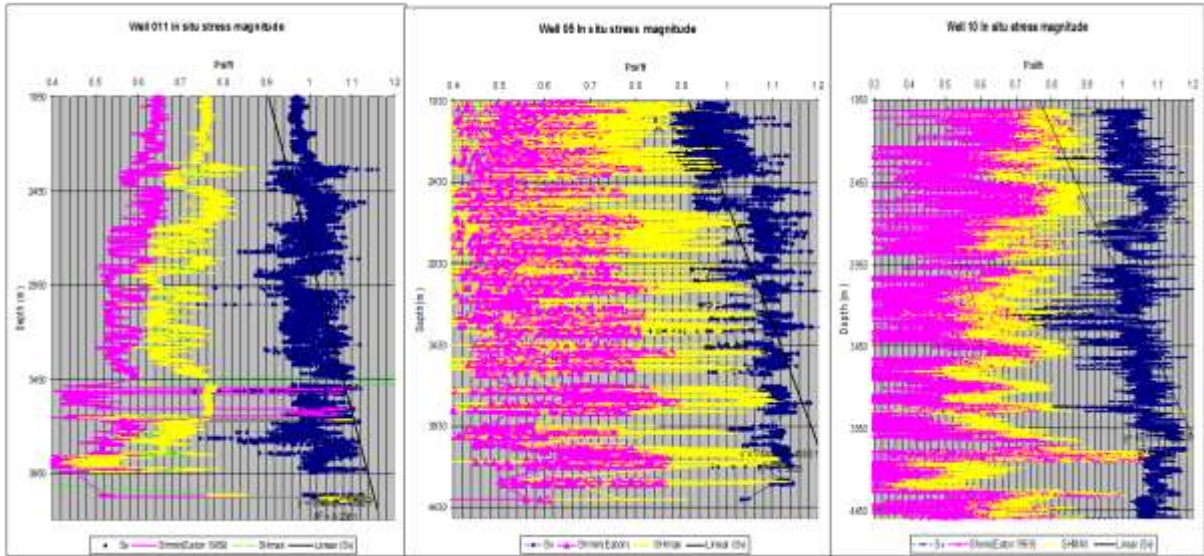


Figure 6 In situ and wellbore stress

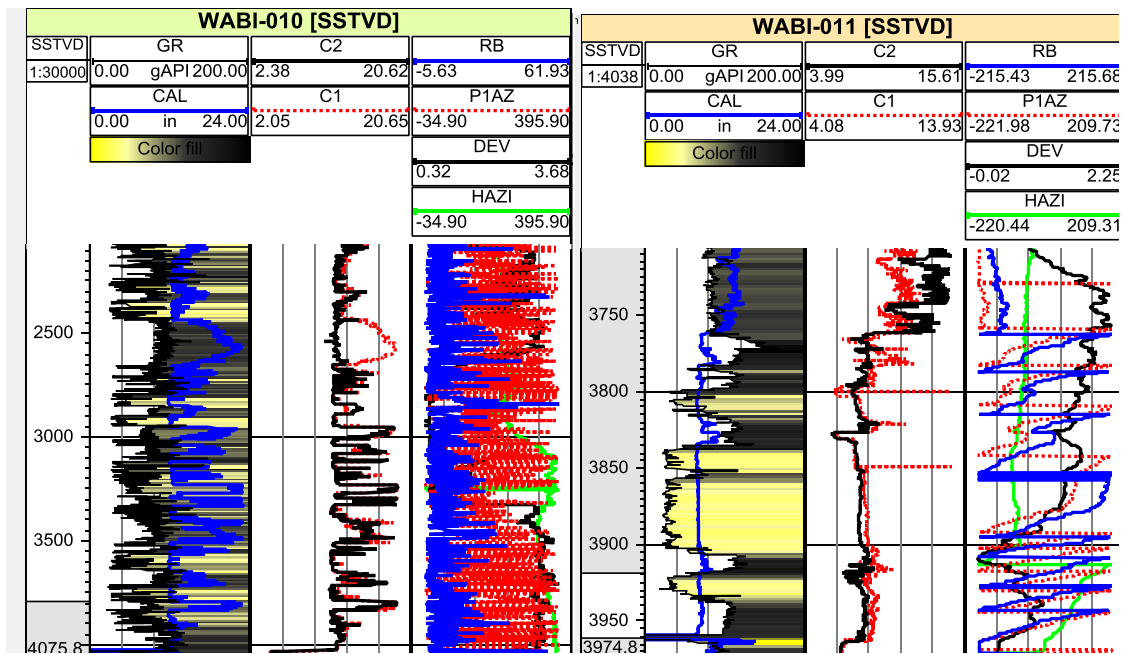


Figure 7 Wellbore breakout log in WABI 010 and WABI 011 wells.

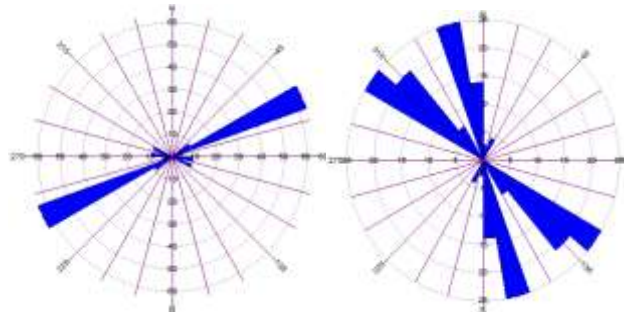


Figure 8 Breakout orientation diagram (a): WABI 11 (b) WABI 10

Table 5 WABI field wellbore breakout data.

Break out top(TVDSS) (m).	Break out bottom(TVDSS) (m)	Breakout length (m)	Loglength analyze (m)	Holedeviation (°).	Breakout Azimuth (°)	MeanBreak outAzimuth (°)	Standard deviation	WSM ranking	σ_{hmin} direction	σ_{Hmax} direction
WABI 10										
2052.7	2054.7	2	2,060.4	0.80	26	15.89	0.59	A	015°	060°
2070.7	2089.2	18.2		0.70	4.75					
2350.6	2351.1	0.5		2.7	22.5					
2359.2	2360.3	1.1		2.4	22.5					
2874.3	2886.5	12.2		0.73	13.70					
2902.3	2903.5	1.2		0.75	12					
3082.8	3083.9	1.1		1.0	48					
3134.9	3135.4	0.5		1.4	18					
3312.5	3313.2	0.7		1.3	35					
3454.2	358.5	4.3		2.9	55.5					
3463.3	3464.1	0.8		3.0	57					
3555.3	363.9	8.6		3.09	53.8					
3586.	3586.8	0.8		2.9	51					
3675.7	3689.4	13.7		3.37	47.5					
3719.4	3722.9	3.5		3.22	38.25					
WABI 011										
3991.4	3998.2	6.8	137.9	0.52	70.29	33.31	9.72	C	033°	123°
4000.5	4001.	0.5		0.4	63					
4004.8	4021.6	16.8		1.45	69					
4041.9	4042.7	0.8		1.8	64					
4053.6	4054.6	1		1.7	64					

Mud weight window for wellbore stability

Wellbore stability analysis involves determining the minimum mud weight (shear failure gradient) required for drilling without causing shear failure and the maximum mud weight required not to cause unintentional tensile fracturing. Maintaining a stable wellbore during drilling requires a mud weight window that is between the shear failure gradient and the fracture gradient. Normal overbalance drilling requires maintaining the mud density above the pore pressure and below the fracture gradient limit. Drilling at mud weights lower than the pore pressure may result in borehole splintering or washout and fracturing will occur if the mud weight is higher than the fracture gradient. Equally drilling at a mud weight lower than the shear failure gradient will cause shear failure. This therefore requires that a safe mud weight window be predicted for safe drilling [39]. The optimum mud weight is the average between the minimum and maximum mud weights. Fig. 9 shows predicted mud weight window for the wells for drilling without borehole collapse and unintentional fracturing of the formation based in isotropic formations. Mud weight window varies with depth across the field due to heterogeneity and anisotropies. A mud window range of 5.0 – 19.0ppg is predicted across the field. In some sections of the wells, the minimum mud weight exceeds the maximum mud weight. The drilling mud weight at such sections should be maintained at fracture gradient limit to avoid the risk of unintentionally fracturing the formation with attendant mud losses which is more dangerous than the breakout formation due to excessively low mud weights. Weak sections with very low shear strength may be strengthened to prevent collapse.

Drilling trajectory

Geosteering the optimum well path requires the most stable trajectory not to cause stress re-orientation, increase the wellbore hoop (tangential) stress and risk of wellbore instability. A vertical well will be most stable in isotropic formations. However, in anisotropic formations where a horizontal lateral section is required to intersect natural fractures and enhance the effective permeability and hence producibility, the minimum horizontal stress direction is recommended. In this study field, the direction of the minimum horizontal stress azimuth of approximately 024° is the most stable. This means that fractures will form and propagate in an orthogonal plane in a northwest- southeast direction. Drilling across the fault could cause anisotropies, reactivation, slip and rotation of the in situ stresses thereby causing instability. Under this condition, the well path will be more stable if drilled in the differential stress ($\sigma_1 - \sigma_3$) direction as suggested by [16] rather than the minimum horizontal stress azimuth.

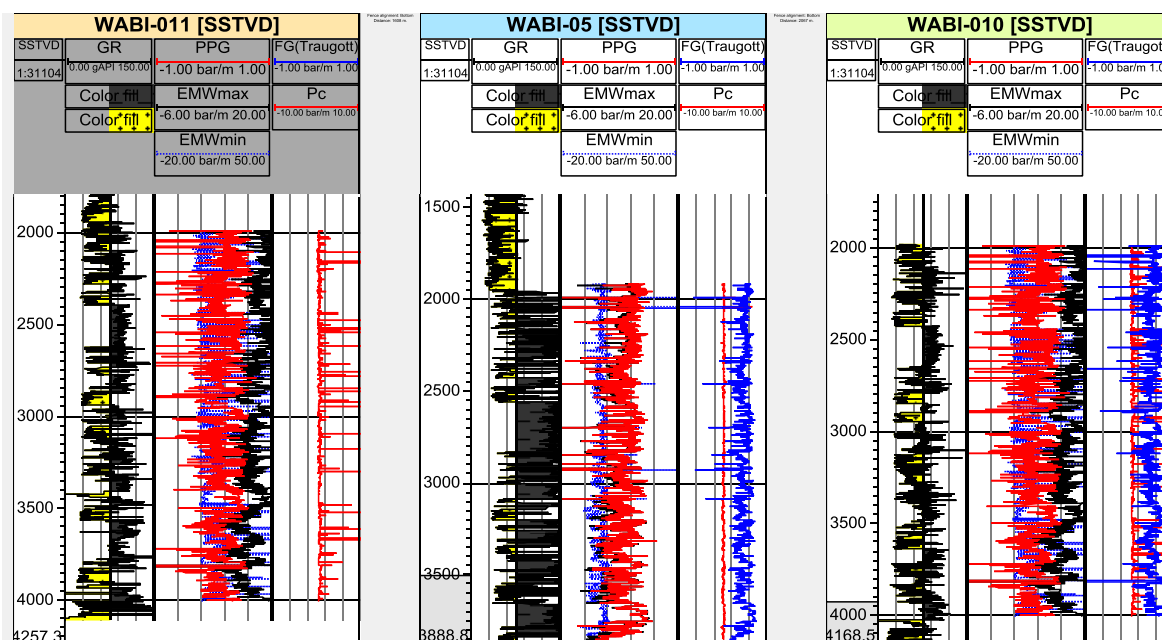


Figure 9 Mud weigh window for wells across the field

Hydraulic fracturing

The fracture gradient predicted for wells in the field can be applied in stimulation pressure design for hydraulic fracturing to improve permeability and optimize production. Weak sections with very low shear strength may require gravel packing to prevent sanding and propant selection should be based on compressibility data. Hydraulically stimulated fractures in horizontal laterals are recommended to be placed vertical and perpendicular to the minimum horizontal stress direction.

V. Conclusion

Knowledge of in situ stress, mechanical properties of reservoir and cap rocks, pore pressure and fault system are key in designing stable and productive wells to optimize production and enhance recovery. In this study, the vertical stress increases vertically and laterally across the field due to variation in the density of sub-crustal materials, while the moduli of rigidity, bulk and matrix volume, bulk and grain compressibility decreases with depth. Generally, there is an increase in elastic modulus of the rocks with depth due to increase in confining stress. Mud weight window varies between 5.0 to 19.0ppg with depth across the field due to heterogeneity and anisotropy. The direction of the minimum horizontal stress was approximately 024° azimuth in a general northeast-southwest implying that fractures will form and propagate in an orthogonal plane in a northwest- southeast direction. Results of the work may be used as a guide in drilling planning and production optimization.

Acknowledgements

Data for this study were provided by Total E&P Nig. Ltd, through the Department of Petroleum Resources, Lagos, to whom the authors are grateful. We also acknowledge Schlumberger for the Petrel software domiciled in the Workstation of the Department of Geology, University of Port Harcourt was used in the course of this work.

References

- [1]. H. Kulke, Nigeria, in, Kulke, H., ed. Regional Petroleum Geology of the World. Part II: Africa, America, Australia and Antarctica, (Berlin, Gebrüder Borntraeger 1995) 143-172.
- [2]. D. Moos, Geomechanics Applied to Drilling Engineering. In Lake, W. L and Mitchel, R. F. eds. Drilling Engineering (2006) Vol. II pp 1 – 173.
- [3]. J. Cook, A.F. Rene, K. Hasbo, S. Green, A. Judzis, J.W. Martiu, R. Suarez-Rivera, H.Jorg, P. Hooyman, D.Lee, S. Noerth, C. Sayers, N.Koutsabelloulis, R. Marsden, M.G. Stage, and C.P. Tan, Rocks matter: Ground truth in geomechanics. Oil Review, 2007, 36 – 55.
- [4]. D. Denney, 3D Geomechanical modeling of optimizes drilling in the Llanos Orientales basin, Columbia. Journal of Petroleum Technology, 63 (9), 2011, 86 – 88.
- [5]. W. Al-Kattan and N.J. Al-Ameri, Estimation of the Rock Mechanical Properties Using Conventional Log Data in North Rumaila Field. Iraqi Journal of Chemical and Petroleum Engineering 13(4), 2012, 27- 33
- [6]. M.O. Eshkalk, S.D. Mohaghegh and S. Esmaila, Geomechanical Properties of Unconventional Shale Reservoirs. Journal of Petroleum Engineering Article ID 961641, 2014, 10 pages <http://dx.doi.org/10.1155/2014/961641>

- [7]. X. Yi, P. P. Valko, and J.E. Russell, Effect of rock strength on the predicted onset of sand production. *International J. of Geomechanics*, 5(1),2005, 86 – 73.
- [8]. M.A. Mohuidin, K. Khan, A. Abdurraheem, A.Al-Majed, and M.R. Awal, Analysis of wellbore instability in vertical, directional and horizontal wells using field data. *Journal of Petroleum Science and Engineering*, (55) 2006, 83 – 92.
- [9]. B. Pasic, N. Gaurena-Medimurec, and D. Mantanovic, 2007. Wellbore instability: Causes and Consequences. *Rudarsko-geolosko-naftni-zbornik*, (19), 2007, 87 -98.
- [10]. H.M. Abbas, M. Warlick, C.H. Pardo, R.M. Khan, A.M. Al-Tahini, D.A. Al-Shehri, H.H. Al-Badairy, M.A. Al-Shobaili, T. Finkbeiner, T. and S. Perumalla, Evaluation of wellbore stability during drilling and production of open hole horizontal wells in a Carbonate field. *Saudi Aramco Journal of Technology*: Fall 2009, 44 – 55.
- [11]. S. Mondal, G. Karthykeyan, and B.K. Patel, 2013. Predrill wellbore stability analysis using rock physical parameters for a deep water high angle well: a case study. *Proc. 10th Biennial International conference and exposition*, Kochi, (Paper No. 046), 2013, 1 - 8.
- [12]. R.A. Farquhr, S.M. Somerville, and B.G.D. Smart, Porosity as a geomechanical indicator: an application of core log data and rock mechanics. *SPE 26454*, 1994.
- [13]. N. Tan, *Fracture Pressure. -Well design*. New Mexico University of Technology: Spring Lecture Monograph.2013, 1 – 34.
- [14]. V. Azizi and H. Memarian, Estimation of Geomechanical Parameters of Reservoir Rocks, using Conventional Porosity Log. *Proc. 4th Asian Rock Mechanics Symposium, Rock Mechanics in Underground Construction*. Retrieved on: 17 July 2015
- [15]. P. Paul, and M. Zoback, Wellbore stability study for the SAFOD borehole through the San Andreas Fault. *SPE 102781 PP 394 – 408*.2008.
- [16]. A. Dosumu, *The gamblers ruin – The driller’s albatross*. University of Port Harcourt Inaugural Lecture Series, No. 115. 2014
- [17]. K.C. Short, and A. J. Stäuble, Outline of geology of Niger Delta: *American Association of Petroleum Geologists Bulletin*, (51) 1967, 761-779.
- [18]. B.D. Evamy, J. Haremboure, P. Kamerling, W.A. Knaap, F.A. Molloy, and P.H. Rowlands, Hydrocarbon habitat of Tertiary Niger Delta: *AAPG Bull.*, (62) 1978, 277-298.
- [19]. P. Stacher, Present understanding of the Niger Delta hydrocarbon habitat, in, Oti, M.N., and Postma, G., eds., *Geology of Deltas: (Rotterdam, A.A. Balkema, 1995)*, 257-267.
- [20]. R.A. Plumb and S.H. Hickman, S.H. Stress-induced borehole elongation: A comparison between the four-arm dipmeter and the borehole televiewer log in Auburn Geothermal Well. *Journal of Geophysical Research*, 90 (B7), 1985, 5513 – 5521.
- [21]. D.I. Gough, and J.S. Bell, Stress Orientations from Borehole Wall Fractures with Examples from Colorado, East Texas, and Northern Canada. *Can. J. Earth Sci.* (19) 1982, 1958-1970.
- [22]. J. Reinecker, M. Tingay, and B. Muller, Borehole breakout analysis from four arm caliper logs. *World Stress Map Project: Guidelines; Four arm caliper logs*, 2003 Pp. 1 – 5.
- [23]. M. Haftan, B. Boholi, M. Eliassi and B. Talebi, 2008. In-Situ Stress Determination in Sabalan Geothermal Reservoir. 2nd IASME/WWSEAS International Conference on GEOLOGY and SEISMOLOGY (GES'08) Cambridge, UK, February 23-25. 2008.88-93
- [24]. G. Harelan, and R. Nygård, Calculating unconfined rock strength from drilling data. *Proc. 1st Canada-U.S. Rock Mechanics Symposium, Vancouver, British Columbia, Canada, 27–31 May 2007*, 34-41
- [25]. K. Haug, R. Nygaard and D. Keith, Evaluation of Stress and Geomechanical Characteristics of a Potential Site for CO₂ Geological Storage in Central Alberta, Canada. *Breaking Grounds in the Nation’s Capital. Diamond Jubilee Ottawa paper*. 2007, 8p. Accessed online July 2, 2015
- [26]. S. Eyinla and Oladunjoye, Estimating Geo-Mechanical Strength of Reservoir Rocks from Well Logs for Safety Limits in Sand-Free Production. *Journal of Environment and Earth Science*. 4(20), 2014, 38-43
- [27]. M.L. Greenberg, and J.P. Castagna, Shear wave velocity estimation in porous rocks. *Theoretical formulations: Preliminary verification and application. Geophysical Prospecting* (40), 1993, 195 – 209.
- [28]. M.E. Jones, M.J. Leddra, A.S. Goldsmith, and D. Edwards, D. The geomechanical characteristics of reservoirs and reservoir rocks. *HSE - Offshore Technology Report, OTH 90, 333, 1992*, 1 – 202.
- [29]. Schlumberger, *Log interpretation principles/applications*. (Schlumberger Educational Services: Houston, 1989) 1-1 – 13-19
- [30]. M.A. Biot, General theory of three - dimensional consolidation. *J. Appl. Phys.* 12 (2), 1941, 155–164. <http://dx.doi.org/10.1063/1.1712886>.
- [31]. E.R. Crain, and D. Holgate, Digital log to mechanical rock properties for stimulation design. *Geoconvention: Focus*.2004. 1-9.
- [32]. G.H. McNally, Estimation of coal measures rock strength using sonic and neutron logs. *Geoexploration*, (24)1987, 381 – 395.
- [33]. M. Lal, *Shale Stability: Drilling Fluid Interaction and Shale Strength*. SPE Asia Pacific Oil and Gas Conference and Exhibition Paper, Jakarta, 20–22 April. 1999, SPE 54356.
- [34]. G. R.Coates and S.A. Denoo, Mechanical properties programme using borehole analysis and Mohr circle. *SPWLA 22nd Annual Logging Symposium*, 1981
- [35]. J.S. Bell, Practical methods for estimating in-situ stresses for borehole stability applications in sedimentary basins: *Journal of Petroleum Science and Engineering*, 38(3-4), 2003, 111–119.
- [36]. R.L. Dart, In situ stress analysis of the wellbore breakouts from Oklahoma and Texas Panhandle. In *Evolution of sedimentary basins – Anadarko*. USGS Bulletin 18866-F, 1990, f1 – f 28.
- [37]. K.V. Mardia, *Statistics of directional data*. New York: Academic press, 1972.
- [38]. B. Sperner, B. Muller, O. Heidbach, D. Delvaux, D. Reinecker and K. Fuchs, Tectonic stress in the earth’s crust. *Advances in the World stress map project*. In Nieuwland, D.(ed). *New insights into structural interpretation and modeling*, Geological Society of London Special Publication, (212), 2003, 101 – 116.
- [39]. J. Zhang, Borehole stability analysis accounting for anisotropies in drilling to weak bedding planes. *International Journal of Rock Mechanics and Mining Sciences*, 60, 2013, 160 – 170.
- [40]. A.I. Opara, Estimation of multiple sources of overpressures using vertical effective stress approach: a case study of Niger Delta. *Petroleum and Coal*, 53(4) 2011, 302 – 314.
- [41]. S. O’Connor, R. Swarbrick, B. Pindar, O. Lucas, F. Adesanya, A. Adedayo, K. Nwankwoagu, A. Edwards, J. Heller, P. Kelly, Pore pressure prediction in the Niger Delta – Lessons learnt from regional analysis. *NAPE, Lagos Conference paper extended abstract*. 2011
- [42]. S. Banerjee, and S. Muhuri, S. Applications of geomechanics – based restoration in structural analysis along Passive Margin Settings – Deep Water Niger Delta example. In *New Understanding of the Petroleum System of Continental Margins of the World*.2013.
- [43]. P. Lehner, and P.A.C. De Ruiter, Structural history of Atlantic Margin of Africa: *American Association of Petroleum Geologists Bulletin*, 61: 1977, 961-981.

- [44]. T. Engelder, Stress regimes in the lithosphere. Princeton: Princeton University Press, 1993) 457.
- [45]. J.B. Wright, Fracture system in Nigeria and initiation of fracture zones in the South Atlantic. *Tectonophysics*, 34, 1978, 13 – 47.
- [46]. E.O. Adewole, and D. Healy, Quantifying in situ horizontal stress in the Niger delta basin, Nigeria, *GSTF, J. of Engineering Technology (JET)*, 2(3) .2013